Plasticity of *Mycobacterium tuberculosis* NADH dehydrogenases and their role in virulence

Catherine Vilchèze[a,b], Brian Weinrick[a,b,1], Lawrence W. Leung[c], and William R. Jacobs Jr.[a,b,2]

[a]Howard Hughes Medical Institute, Albert Einstein College of Medicine, Bronx, NY 10461; [b]Department of Microbiology and Immunology, Albert Einstein College of Medicine, Bronx, NY 10461; and [c]Gray Box Biology LLC, New York, NY 10027

Contributed by William R. Jacobs Jr., January 4, 2018 (sent for review December 12, 2017; reviewed by Eric L. Nuermberger and Harvey Rubin)

Worldwide control of the tuberculosis (TB) epidemic has not been achieved, and the latest statistics show that the TB problem might be more endemic than previously thought. Although drugs and a TB vaccine are available, TB eradication faces the challenges of increasing occurrences of multidrug-resistant and extensively drug-resistant *Mycobacterium tuberculosis* (*Mtb*) strains. To forestall this trend, the development of drugs targeting novel pathways is actively pursued. Recently, enzymes of the electron transport chain (ETC) have been determined to be the targets of potent antimycobacterial drugs such as bedaquiline. We focused on the three NADH dehydrogenases (Ndh, NdhA, and Nuo) of the *Mtb* ETC with the purpose of defining their role and essentiality in *Mtb*. Each NADH dehydrogenase was deleted in both virulent and BSL2-approved *Mtb* strains, from which the double knockouts Δ*ndh*Δ*nuoAN* and Δ*ndhA*Δ*nuoAN* were constructed. The Δ*ndh*Δ*ndhA* double knockout could not be obtained, suggesting that at least one type II NADH dehydrogenase is required for *Mtb* growth. Δ*ndh* and Δ*ndh*Δ*nuoAN* showed growth defects in vitro and in vivo, susceptibility to oxidative stress, and redox alterations, while the phenotypes of Δ*ndhA*, Δ*nuoAN*, and Δ*ndhA*Δ*nuoAN* were similar to the parental strain. Interestingly, although Δ*nuoAN* had no phenotype in vivo, Δ*ndh*Δ*nuoAN* was the most severely attenuated strain in mice, suggesting a key role for Nuo in vivo when Ndh is absent. We conclude that Ndh is the main NADH dehydrogenase of *Mtb* and that compounds that could target both Ndh and Nuo would be good candidates for TB drug development.

NADH | virulence | essentiality | tuberculosis | dehydrogenase

Tuberculosis (TB), a disease caused by the bacillus *Mycobacterium tuberculosis* (*Mtb*), remains one of the leading causes of mortality due to a single infectious agent. Despite chemotherapy and the bacillus Calmette–Guérin vaccine, worldwide incidences of this disease persist, while multidrug-resistant (MDR) and extensively drug-resistant (XDR) *Mtb* strains have emerged, rendering TB control even more challenging. The current TB pharmacopeia is divided into three categories: first-line, second-line, and third-line TB drugs. Drug-susceptible TB cases are treated with the first-line TB drugs isoniazid (INH), rifampicin (RIF), ethambutol (EMB), and pyrazinamide (PZA). These drugs target the mycobacterial cell wall (INH and EMB) and transcription (RIF), while the target of PZA is still under investigation. The second-line TB drugs used to treat drug-resistant cases include drugs targeting the DNA gyrase (fluoroquinolones), protein synthesis (aminoglycosides and cyclo-peptides), or the cell wall (thioamides and cycloserine) (1). To fight the TB drug resistance pandemic, novel pathways for drug development need to be explored. One of the most promising new TB drugs is bedaquiline, which targets the oligomeric c ring of the F_1F_o-ATP synthase complex. ATP synthesis catalyzed by the F_1F_o-ATP synthase is driven by the protonmotive force (*pmf*) generated by the electron transport chain (ETC). Other components of the oxidative phosphorylation machinery are also showing promise for drug development. The proton-pumping cytochrome *bc1* complex is targeted by a novel drug in development, Q203 (Qurient, Infectex) (2). Q203 was shown to be cidal against *Mtb* when combined with inhibition of the cytochrome *bd* oxidase activity (3). SQ109 (Sequella) is thought to disrupt the biosynthesis of the electron carrier menaquinone and the *pmf* through uncoupling activity (4). The *pmf* generated by the ETC is an essential element for the survival of any organism under both aerobic and hypoxic growth conditions, which makes this system attractive for drug development (5).

Primary NADH dehydrogenases play a pivotal role in energization of the mycobacterial respiratory chain. *Mtb* has three membrane-bound NADH dehydrogenase complexes that are capable of oxidizing the cofactor NADH into NAD^+ using menaquinone as an electron acceptor. These include the proton-translocating (type I–NDH-1) Nuo complex and two nonproton-pumping (type II) Ndh and NdhA complexes (NDH-2). To assess which NADH dehydrogenase enzyme was the most relevant target for drug design, we deleted each *Mtb* gene or operon encoding these enzymes individually and in tandem and tested the resulting knockout strains in vitro and in vivo for viability. NdhI, which is composed of 14 subunits (NuoA-NuoN, Rv3145-Rv3158), had already been shown dispensable, as transposon insertions had been identified in most of the subunits (6), and the full operon has been deleted from the *Mtb* genome (7). Transposon insertions had also been previously isolated in *ndhA* (*Rv0392c*) (8), but *ndh* (*Rv1854c*) was considered an essential gene, as specific mutations in *ndh* had temperature-sensitive lethal phenotypes in *Mycobacterium smegmatis* (9, 10), transposon insertions in *Mtb ndh* were rare (11), and attempts at deleting *Mtb ndh* had been unsuccessful (12). This report describes the construction of single- and double-NADH dehydrogenase deletion mutants in *Mtb* strains and their phenotypes in vitro and in vivo.

Significance

Tuberculosis drug development remains crucial for countering the spread of drug resistance worldwide. New susceptibilities in metabolic pathways must be identified to find novel drugs to eradicate tuberculosis. The electron transport chain (ETC) is the target of recently developed tuberculosis drugs. To assess whether the NADH dehydrogenases of the ETC would be potential drug candidates, we deleted the genes encoding the three *Mycobacterium tuberculosis* NADH dehydrogenases Nuo, Ndh, and NdhA. We found that although the NADH dehydrogenases were not essential for growth individually, deletion of both *nuo* and *ndh* had the most profound effect on *Mycobacterium tuberculosis* viability and virulence. We propose that screening compound libraries against both Ndh and Nuo will lead to promising drug candidates to fight tuberculosis.

Author contributions: C.V. and W.R.J. designed research; C.V., B.W., and L.W.L. performed research; C.V. analyzed data; and C.V. and W.R.J. wrote the paper.

Reviewers: E.L.N., Johns Hopkins University School of Medicine; and H.R., University of Pennsylvania.

The authors declare no conflict of interest.

[1]Present address: Tuberculosis Research Center, Trudeau Institute, Saranac Lake, NY 12983.

[2]To whom correspondence should be addressed. Email: jacobsw@hhmi.org.

This article contains supporting information online at www.pnas.org/lookup/suppl/doi:10.1073/pnas.1721545115/-/DCSupplemental.

Results

NADH Dehydrogenase Genes Are Individually Dispensable in *Mtb*. The NADH dehydrogenase type I operon, encoded by *nuoAN*, and the two NADH dehydrogenases type II encoded by *ndh* and *ndhA,* were deleted from the *Mtb* strains CDC1551 and mc^{2}6230 (*Mtb* H37Rv ΔRD1Δ*panCD*) using the specialized transduction system (13, 14) and replaced by a γδ(*sacB-hyg*) γδ cassette (Table S1). The hygromycin cassette was excised in each knockout strain to obtain unmarked deletion strains (14). These strains were then confirmed by Southern analysis and by whole-genome sequencing (Fig. S1). The unmarked deletion strains Δ*ndh*, Δ*ndhA*, and Δ*nuoAN* were then used to generate deletions of a second NADH dehydrogenase in each background using the same specialized transduction phages used to generate Δ*ndh* (phAE237), Δ*ndhA* (phAE804), and Δ*nuoAN* (phAE805). The double-knockout Δ*ndh*Δ*nuoAN* and Δ*ndhA*Δ*nuoAN* strains were obtained; however, six independent attempts failed to produce a Δ*ndh*Δ*ndhA* mutant. The Δ*ndh*Δ*nuoAN* and Δ*ndhA*Δ*nuoAN* constructions were confirmed by Southern analysis (Fig. S1). Δ*ndh*Δ*nuoAN* was further confirmed by whole-genome sequencing (Fig. S1). This set of deletion strains demonstrates that the NADH dehydrogenases are not essential individually, but that most likely one type II NADH dehydrogenase is required for the viability of *Mtb* in vitro.

Deletion of NADH Dehydrogenase Genes Affects NADH Dehydrogenase Expression Levels and NADH/NAD$^+$ Ratio. To examine the impact of the deletion mutants on the expression levels of the three NADH dehydrogenase genes in *Mtb*, qPCR was performed using primers to amplify the *ndh, ndhA*, and *nuoH* genes (Fig. 1*A* and Table S2). The levels of *nuo* and *ndhA* expression in Δ*ndh* decreased by 15% and 50%, respectively, compared with WT. Complementation of Δ*ndh* with *Mtb ndh* cloned downstream of the *hsp60* promoter (Table S3) restored *nuo* and *ndhA* expression levels to or above WT expression levels. Deletion of the NADH dehydrogenase type I operon (Δ*nuoAN*) led to overexpression of both type II NADH dehydrogenases, while the double knockouts, Δ*ndh*Δ*nuoAN* and Δ*ndhA*Δ*nuoAN*, overexpressed *ndhA* and *ndh,* respectively. Δ*ndhA* was the only *Mtb* strain with a similar level of *ndh* and *nuo* transcripts compared with the WT strain.

The function of the NADH dehydrogenases is to oxidize NADH into NAD$^+$, the ratio of which reflects the redox state of a cell. Therefore, the NADH/NAD$^+$ ratio was determined for each of the NADH dehydrogenase mutants and found to be increased in the Δ*ndh* and double-knockout strains while remaining similar to WT level in the Δ*ndhA* and Δ*nuoAN* strains (Fig. 1*B*). While the deletion of *ndhA* or *nuoAN* may not induce any major redox perturbation in *Mtb*, the NADH/NAD$^+$ ratio was the most altered when *Mtb* was lacking *ndh*, suggesting that this enzyme has an important function in maintaining the redox status of the cell.

Only Δ*ndh* and Δ*ndh*Δ*nuoAN* Have Growth Defects in Vitro. The five NADH dehydrogenase knockout strains Δ*ndh*, Δ*ndhA*, Δ*nuoAN*, Δ*ndh*Δ*nuoAN*, and Δ*ndhA*Δ*nuoAN* were tested for growth in Middlebrook 7H9-glycerol–OADC (oleic acid, albumin, dextrose, catalase). All of the strains containing *ndh* grew similarly to the WT strain (Fig. 2*A*). In contrast, Δ*ndh* and Δ*ndh*Δ*nuoAN* showed a longer lag phase during growth than WT, although once the strains had reached log phase, the kinetics of growth and the maximum growth rate achieved were similar to WT (Fig. 2*B*). This increased lag phase was resolved in the Δ*ndh*-complemented strain (Fig. 2*B*). This growth delay was reproducible and unlikely due to the inoculation of large volume of nonviable bacteria, as cultures were typically reinoculated while in log phase. In *Salmonella typhimurium* (15) and in *Escherichia coli* (16), the switch to lag phase was shown to generate a transient oxidative stress when cultures were inoculated into freshly oxygenated medium. To test whether deletion of *ndh* or *ndh* and *nuoAN* could increase *Mtb* sensitivity to oxidative stress, we grew the NADH dehydrogenase deletion mutants in Middlebrook 7H9-glycerol–ADS, a medium without catalase, an enzyme that converts hydrogen peroxide to oxygen and water and protects the bacteria against oxidative stress (Fig. 2*C* and Fig. S2). Only the Δ*ndh* and Δ*ndh*Δ*nuoAN* mutants were substantially affected by this growth condition, exhibiting an extended lag phase increased by 9 and 15 d, respectively, compared with growth in medium containing catalase (Fig. 2*B*). The susceptibility of Δ*ndh* and Δ*ndh*Δ*nuoAN* to oxidative stress was confirmed when catalase was added to Δ*ndh* and Δ*ndh*Δ*nuoAN* grown in Middlebrook 7H9-glycerol–ADS, and a reduction in the lag phase was observed for these two mutants (Fig. 2*D*). The defects observed in Δ*ndh* and Δ*ndh*Δ*nuoAN* during these in vitro growth experiments suggest that in addition to its role in the ETC, Ndh might also protect *Mtb* from oxidative stress.

Δ*ndh* and Δ*ndh*Δ*nuoAN* Are More Susceptible to Oxidative Stress Reagents, but Not to Potential NADH Dehydrogenase Inhibitors. The data generated by the growth condition studies led us to investigate the susceptibility of the NADH dehydrogenase mutants to agents generating oxidative stress. Minimum inhibitory concentrations (MIC) were determined for the NADH dehydrogenase mutants against hydrogen peroxide and ascorbic acid, which can generate an oxidative environment in *Mtb* (17). The NADH dehydrogenase mutants had similar levels of susceptibility to hydrogen peroxide as their parental strain, while Δ*ndh* and Δ*ndh*Δ*nuoAN* were slightly more susceptible to ascorbic acid (two- to fourfold) than CDC1551 (Table 1).

We next measured the MICs of compounds that target the NADH dehydrogenase type II, such as trifluoperazine (TPZ; 18), chlorpromazine (CPZ; 18), clofazimine (CFZ; 19), and INH (9, 10), against the NADH dehydrogenase mutants. The two neuroleptic drugs TPZ and CPZ, used in the treatment of psychiatric patients infected with TB in the 1950s, inhibit purified recombinant

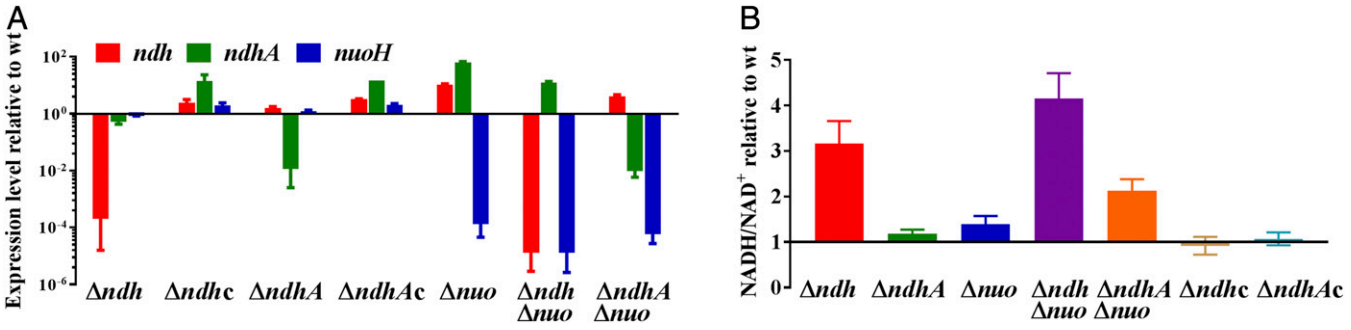

Fig. 1. Deletion of NADH dehydrogenase genes impacts NADH dehydrogenase expression levels and NADH/NAD$^+$ ratio. (*A*) Expression levels of *ndh, ndhA*, and *nuoH* in the NADH dehydrogenase mutants relative to their parental strain CDC1551. (*B*) NADH/NAD$^+$ ratio in NADH dehydrogenase mutants relative to their parental strain CDC1551. In these experiments, the strains were grown in Middlebrook 7H9, supplemented with OADC, glycerol, and tyloxapol to $OD_{600\ nm} \approx 1$. The complemented strains Δ*ndh* pMV361::*ndh* and Δ*ndhA* pMV361::*ndhA* are shown as Δ*ndh*c and Δ*ndhA*c, respectively. Δ*nuo* stands for Δ*nuoAN*. Average of three independent experiments is shown with SD.

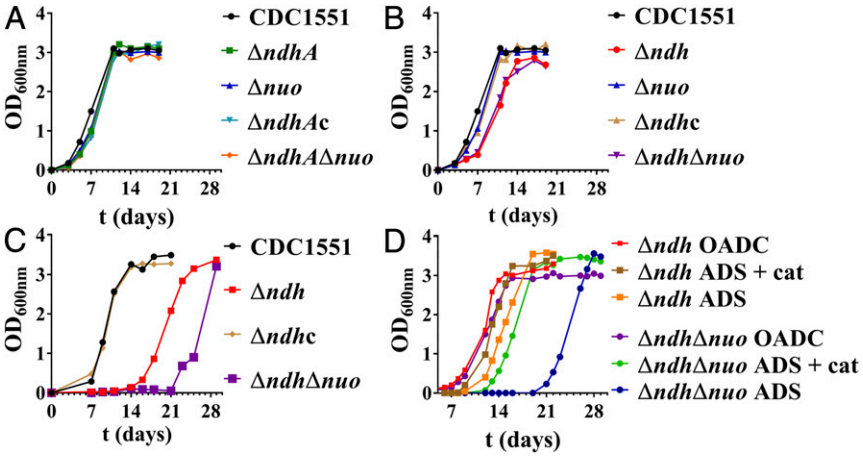

Fig. 2. Δ*ndh* and Δ*ndh*Δ*nuoAN* have growth defect in vitro. The NADH dehydrogenase mutants and their parental strain CDC1551 were grown to midlog ($OD_{600\ nm} \approx 0.8$) and diluted 1/50. Growth was followed by measuring $OD_{600\ nm}$ over time. (*A* and *B*) Growth in Middlebrook 7H9, supplemented with OADC, glycerol, and tyloxapol. (*C*) Growth in Middlebrook 7H9, supplemented with ADS, glycerol, and tyloxapol. (*D*) Growth of Δ*ndh* and Δ*ndh*Δ*nuoAN* in Middlebrook 7H9, supplemented with, glycerol, tyloxapol, and OADC, ADS, or ADS-containing catalase (3 mg/L, same concentration as in OADC). The complemented strains Δ*ndh* pMV361::*ndh* and Δ*ndhA* pMV361::*ndhA* are shown as Δ*ndh*c and Δ*ndhA*c, respectively. Δ*nuo* stands for Δ*nuoAN*. The graphs show single replicates, which are representative of at least two independent experiments.

Ndh and NdhA (18) and had similar MICs across all of the strains tested (Table 1). A low-level (up to fourfold) resistance was observed for Δ*ndh* and Δ*ndh*Δ*nuoAN* against CFZ, a prodrug that requires Ndh for its activation (19), and INH (Table 1).

Δ*ndh* and Δ*ndh*Δ*nuoAN* Have a Late-Growth Defect in Murine Macrophages. Considering that *Mtb* is an intracellular pathogen, we asked whether the in vitro growth defect we had observed with the Δ*ndh* and Δ*ndh*Δ*nuoAN* mutants could be reproduced in murine macrophages. Murine J774 macrophages were infected at a multiplicity of infection of 1 with the NADH dehydrogenase mutants, and growth of the mutants was followed for 4 d (Fig. 3). None of the mutants had any growth defect compared with the parental strain early on, but a significant ($P < 0.05$) growth defect was observed at the last day of infection (day 4) for Δ*ndh* and Δ*ndh*Δ*nuoAN* (Fig. 3*A*). This suggested that these two mutant strains might have an in vivo growth defect phenotype.

Δ*ndh* and Δ*ndh*Δ*nuoAN* Are Attenuated in Vivo. Immunocompetent mice were infected i.v. with the NADH dehydrogenase mutants at a dose of ~10^6 bacteria to assess both the in vivo growth and the virulence of the NADH dehydrogenase mutants. Δ*ndh*, Δ*ndhA*, Δ*nuoAN,* and Δ*ndhA*Δ*nuoAN* grew comparably to the WT strain in the lungs (Fig. 4*A*) and spleens (Fig. 4*B*) of infected mice. Burden of Δ*ndh*Δ*nuoAN* failed to increase in the lungs of infected mice, and, in the spleen, the Δ*ndh*Δ*nuoAN* titer dropped drastically after the first 4 wk of infection. In parallel, the survival study (nine mice per group; Fig. 4*C*) showed that the mice infected with the parental strain, Δ*ndhA*, Δ*nuoAN,* and Δ*ndhA*Δ*nuoAN*, died in the same time range, while the mice infected with Δ*ndh* or Δ*ndh*Δ*nuoAN* all survived. To further evaluate the virulence defect of Δ*ndh* and Δ*ndh*Δ*nuoAN* observed during the survival experiment, three mice infected with Δ*ndh* or Δ*ndh*Δ*nuoAN* from the survival experiment were euthanized to determine lung and spleen bacterial burdens at 61 wk postinfection. The mice infected with Δ*ndh* had similar spleen burden at 61 wk compared with week 12 and a higher burden in the lungs at week 61 (Fig. 4*D*). The lung burden of the mice infected with Δ*ndh*Δ*nuoAN* had not changed at 61 wk compared with week 12, but the spleen burden was near undetectable levels at 61 wk. Pathology revealed that the lungs of mice infected with Δ*ndh* had widespread chronic scattered granulomatous inflammation with high numbers of lymphocytes both in the inflammation and around vessels (Fig. 4*E*). In contrast, the Δ*ndh*Δ*nuoAN*-infected lung samples had very little evidence of inflammation, which represented less than 5% of the lung area and was histiocytic and lymphocytic. The lack of virulence of Δ*ndh* and Δ*ndh*Δ*nuoAN* led us next to examine the possibility of protection against virulent *Mtb*. The six remaining mice initially infected with Δ*ndh* or Δ*ndh*Δ*nuoAN* from the survival experiment were then infected i.v. with a high dose of WT *Mtb* H37Rv (5×10^6 bacteria). Following the H37Rv challenge, the six mice initially infected with Δ*ndh* had a median survival of 37 d. Three of the six mice initially infected with Δ*ndh*Δ*nuoAN* had a median survival of 98 d following H37Rv challenge, and at 135 d post H37Rv challenge, the other three mice had to be euthanized due to dermatitis. These data establish Δ*ndh*Δ*nuoAN* as the most attenuated NADH dehydrogenase strain in vivo.

To further assess the in vivo virulence defect of the Δ*ndh* and Δ*ndh*Δ*nuoAN* mutants, a low-dose aerosol infection of immunocompetent mice was performed. Mice were euthanized at 1, 3, and 8 wk to determine lung (Fig. 5*A*) and spleen (Fig. 5 *B* and *D*) bacterial burdens. Δ*ndh*Δ*nuoAN* mutant was the most attenuated strain, although it did grow in both organs. The Δ*ndh* mutant grew better than the Δ*ndh*Δ*nuoAN* mutant in both organs but less than the WT strain. Pathology examination of the lung tissues at 8 wk postinfection (Fig. 5*C*) showed that the mice infected with CDC1551 or Δ*ndh* had small to large nodular to diffuse aggregates of large macrophages admixed with lymphocytes and, occasionally, a small amount of necrotic debris multifocally. These histologic findings were typical of *Mtb* infection and filled alveolar spaces and obscured normal pulmonary architecture. The lungs of the mice infected with Δ*ndh*Δ*nuoAN* exhibited the fewest lesions, with small to moderate numbers of lymphocytes admixed with reduced numbers of macrophages, rare plasma cells, and neutrophils multifocally surrounding bronchioles.

In summary, the Δ*ndhA*, Δ*nuoAN,* and Δ*ndhA*Δ*nuoAN* strains are as virulent as the parental strain. *Mtb* strains lacking *ndh* are attenuated for growth and virulence in mice.

Table 1. Susceptibility of NADH dehydrogenase mutants to drugs and oxidative stress agents

Strain/MIC	Ascorbic acid (mM)	H_2O_2 (mM)	CPZ (mg/L)	TPZ (mg/L)	CFZ (mg/L)	INH (mg/L)
CDC1551	1.0	0.5	12.5	25	0.6–1.25	0.03
Δ*ndh*	0.25–0.5	0.25	12.5	25	2.5	0.06–0.12
Δ*ndh* pMV361::*ndh*	1.0–2.0	0.5	Not done	Not done	1.25	0.03
Δ*ndhA*	1.0	0.25–0.5	12.5	12.5	0.6–1.25	0.03
Δ*nuoAN*	1.0	0.5	25	25	0.6–1.25	0.03
Δ*ndh*Δ*nuoAN*	0.5	0.25	25	12.5–25	2.5	0.12
Δ*ndhA*Δ*nuoAN*	1.0	0.5	12.5–25	25	0.6–1.25	0.03–0.06

MICROBIOLOGY

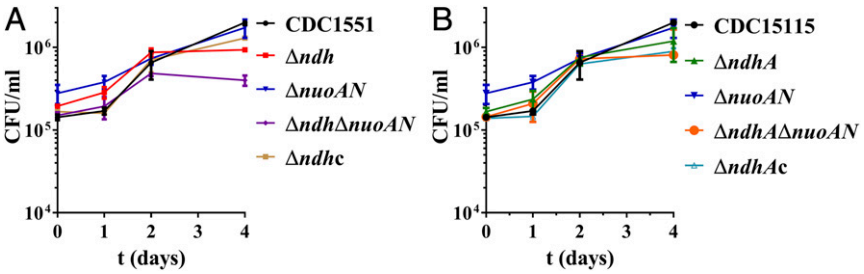

Fig. 3. Δ*ndh* and Δ*ndh*Δ*nuoAN* have a late growth defect in macrophages. J774 macrophages were infected at an MOI (multiplicity of infection) of 1 with CDC1551 or the NADH dehydrogenase mutants. At 1, 2, and 4 d postinfection, macrophages were lysed and plated to determine bacterial cfu. The complemented strains Δ*ndh* pMV361::*ndh* and Δ*ndhA* pMV361::*ndhA* are shown as Δ*ndh*c and Δ*ndhA*c, respectively. The average of two independent experiments done in duplicate is shown with SD.

Discussion

Of the three NADH dehydrogenases present in *Mtb,* only *ndh* encoding the type II NADH dehydrogenase Ndh had been previously described as an essential gene (11, 12). In this study, we show that none of the NADH dehydrogenases are essential in vitro or in vivo, highlighting the need to validate high-throughput transposon essentiality screening with detailed gene-deletion and gene-silencing studies. The failure to obtain the double-deletion mutant Δ*ndh*Δ*ndhA* suggests that *Mtb* requires the presence of at least one type II nonproton-translocating NADH dehydrogenase for growth. The nonproton-translocating activity of these enzymes may be an important feature in allowing *Mtb* to maintain an energized membrane in the absence of growth using lower-efficiency complexes. For example, coupling NDH-2 to cytochrome *bd* would allow *Mtb* to run respiration coupled to nonproton-pumping complexes, and therefore electron flow would not be impeded by *pmf* backpressure in the absence of growth and high rates of ATP synthesis (proton consumption) (20). When NdhA is the only NADH dehydrogenase type II present in *Mtb,* the strain (Δ*ndh*) is impaired for growth in vitro, more susceptible to oxidative stress, and is less virulent in vivo. When NdhA is the only NADH dehydrogenase present in *Mtb,* the strain (Δ*ndh*Δ*nuoAN*) has the most drastic growth-defect phenotype in vitro and in vivo, suggesting a compensatory role for Nuo in the absence of Ndh. In contrast, when Ndh is the only NADH dehydrogenase present in *Mtb,* the strain (Δ*ndhA*Δ*nuoAN*) has no growth defect in vitro or in vivo. The data designate Ndh as the relevant NADH dehydrogenase in vitro and in vivo. Although the Δ*nuoAN* mutant had no phenotype in vitro or in vivo, the severely attenuated phenotype of the Δ*ndh*Δ*nuoAN* strain compared with the Δ*ndh* strain in mice reveals that Nuo may play an important role in the virulence of *Mtb*. Previously, the deletion of a single subunit of the *nuo* operon, *nuoG*, in *Mtb* resulted in a proapoptotic phenotype in human macrophages and increased survival in mice (21). The authors observed no growth defect of the Δ*nuoG* mutant in vitro but a significant reduction in bacterial load in the lungs (although not in the spleen or liver) of immunocompetent mice infected i.v. compared with mice infected with WT *Mtb*. Furthermore, a *nuoG* deletion in the bacillus Calmette–Guérin Δ*ureC::hly* vaccine candidate strain (22) increased vaccine safety (23). Deletion of *nuoG* in bacillus Calmette–Guérin Δ*ureC::hly* led to enhancement of apoptosis and autophagy, two immune cellular pathways that are intimately linked with *Mtb* survival and eradication in the host, and downstream enhancement of anti-*Mtb* immune responses. The molecular basis for the discrepancies between our Δ*nuoAN* mutant and the phenotypes observed with the deletion of a single subunit of *nuo* will require additional studies to elucidate.

Although *ndh* is found in all mycobacteria, *ndhA* is absent in some mycobacterial species such as *M. smegmatis, M. abscessus*, and *M. leprae*, suggesting a nonpivotal role for *ndhA* in the presence of *ndh.* Questions remain as to the presence of two NADH dehydrogenases type II in *Mtb*. Are *ndh* and *ndhA* redundant or required for specific growth conditions? The fact that Δ*ndh* and Δ*ndhA* grew in vitro and in vivo shows that both enzymes are functional, confirming previous biochemical data (24). Interestingly, when grown in vitro, we noticed that the Δ*ndh* strain showed a longer lag time compared with WT or Δ*ndhA*. Lag phase is

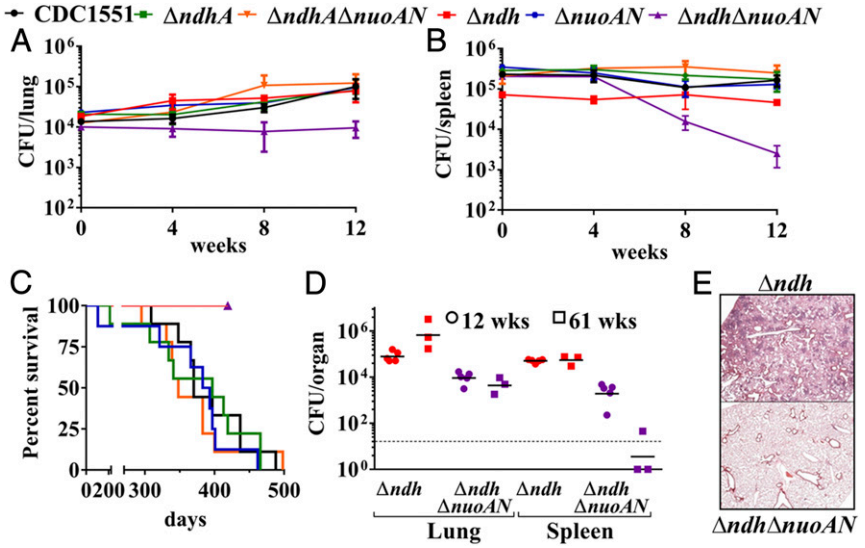

Fig. 4. Δ*ndh* and Δ*ndh*Δ*nuoAN* are avirulent in immunocompetent mice infected intravenously. (*A* and *B*) Lung and spleen burdens of infected C57BL/6 mice at day 1, weeks 4, 8, and 12 (five mice per group and per time point). (*C*) Survival of infected C57BL/6 mice (nine mice per group). (*D*) Three C57BL/6 mice infected with Δ*ndh* and Δ*ndh*Δ*nuoAN* from the survival experiment shown in *C* were euthanized at 61 wk (squares) postinfection to determine their lung and spleen burdens and are compared with the 12-wk organ burdens (circles). cfu counts in lungs and spleen are shown for each individual mouse, and geometric mean is indicated for each group. The limit of detection is indicated by a dotted line. (*E*) Lung tissue sections of C57BL/6 mice infected with Δ*ndh* (*Top*) or Δ*ndh*Δ*nuoAN* (*Bottom*) at 61 wk postinfection were stained with hematoxylin/eosin and observed at a magnification of 2.5×.

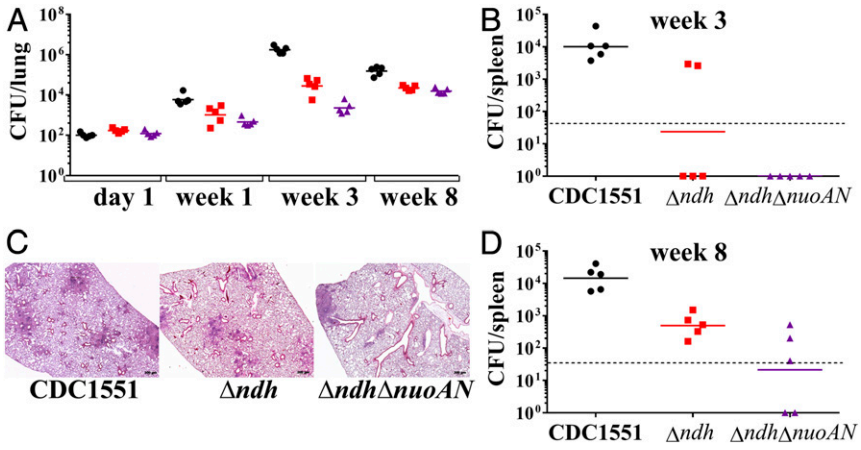

Fig. 5. The growth of Δ*ndh* and Δ*ndh*Δ*nuoAN* is attenuated in immunocompetent mice infected via the aerosol route. C57BL/6 mice were infected with CDC1551 (black circles), Δ*ndh* (red squares), and Δ*ndh*Δ*nuoAN* (purple triangles) via a low-dose (~100 bacilli) aerosol. Lungs (*A*) and spleens (*B* and *D*) were collected, homogenized, and plated to determine organ bacterial burden at 1, 3, and 8 wk postinfection. cfu counts in lungs and spleen are shown for each individual mouse, and geometric mean is indicated for each group. The limit of detection is indicated by a dotted line. (*C*) Lung tissue sections at 8 wk postinfection were stained with hematoxylin/eosin and observed at a magnification of 2.5×.

often considered as the time required by a bacterium to adapt to a new growth condition. Jacques Monod had suggested that the lag time per phase might reflect "an insufficient supply of metabolite(s) or the state of inactivity of an enzyme" (ref. 25, p. 387). It may suggest that, although NdhA is an active NADH dehydrogenase during log phase, its ability to oxidize NADH into NAD^+ might be reduced during lag phase. We did not find an in vitro growth condition where *ndhA* was required, but it is possible that *ndhA* might be necessary for growth with specific nutrient or oxygen conditions. In mice, Δ*ndhA* had no phenotype, while Δ*ndh* displayed a virulence defect. We hypothesize that the oxygen environment in the mouse lung might impair Δ*ndh.* We had previously shown that *ndh* and *ndhA* modulate oxygen consumption differently and both at a slower rate than the parental strain (26). As the level of oxygen decreased, Δ*ndhA* slowed down its oxygen consumption faster than Δ*ndh*, suggesting that Δ*ndhA* controls its respiration and conserves oxygen better than Δ*ndh*.

Enzymes of the ETC-mediating oxidative phosphorylation in *Mtb* are validated drug targets (e.g., ATP synthase, cytochrome bc_1). The NADH dehydrogenase Ndh has no homolog in humans, so *Mtb* Ndh inhibitors could be developed with limited toxicity risk. One consequence of inhibiting Ndh is an increase in the $NADH/NAD^+$ ratio toward a higher reducing potential. Because redox homeostasis is important for the survival of cells in a slowing–replicating state (27, 28), Ndh inhibitors might also be good candidates to target persister or dormant *Mtb* bacteria. In that context, new Ndh inhibitors have been synthesized and shown to have antimycobacterial activity under aerobic and hypoxic conditions against both drug-susceptible and drug-resistant *Mtb* strains (29). Furthermore, redox homeostasis is also an important factor in drug activity and resistance, since many drugs against *Mtb* are prodrugs activated via a reductive process. INH is activated by the catalase peroxidase KatG to form an isonicotinoyl radical that reacts with NAD^+ yielding an INH-NAD adduct (30, 31). It had been previously shown by us and others that mutations in *ndh* led to resistance to INH in mycobacteria (32). *M. smegmatis* and *Mycobacterium bovis* bacillus Calmette–Guérin *ndh* mutants are 20-fold and up to sixfold more resistant to INH, respectively. We had postulated that INH resistance in *M. smegmatis* and *M. bovis* bacillus Calmette–Guérin *ndh* mutants was due to an increase in cellular NADH concentration, which competitively inhibited the binding of the INH-NAD adduct to the NADH-dependent enoyl–ACP reductase InhA (10). The *Mtb* NADH dehydrogenase deletion strains Δ*ndh* and Δ*ndh*Δ*nuoAN* had $NADH/NAD^+$ ratios three to four times higher than their parental strain CDC1551, so we expected them to be INH-resistant, yet they had only very low-level resistance to INH (two- to fourfold). The difference between the phenotypes of the *Mtb*, *M. smegmatis*, and *M. bovis* bacillus Calmette–Guérin Pasteur *ndh* mutants in regard to INH resistance might reflect the NADH concentration in the different mycobacterial species. In *M. smegmatis,* the highly INH-resistant (20-fold) *ndh* mutants had NADH concentrations approaching 2 mM, while the NADH concentrations in the low-level INH-resistant *ndh* mutants of *M. bovis* bacillus Calmette–Guérin were between 0.6 and 0.7 mM (10). In *Mtb*, Δ*ndh*, and Δ*ndh*Δ*nuoAN*, NADH concentrations never exceeded 0.3 mM. We hypothesize that the increase in NADH concentration in *Mtb*, Δ*ndh*, and Δ*ndh*Δ*nuoAN* might not be sufficiently high to efficiently prevent InhA inactivation by the INH-NAD adduct in *Mtb*.

Inhibitors of the NADH dehydrogenases type II such as TPZ and CPZ have good activity against *Mtb* both in vitro and in vivo (24). When tested against the Δ*ndh* and Δ*ndhA* strains, both TPZ and CPZ had similar MIC, confirming that TPZ and CPZ inhibit Ndh and NdhA equally. CFZ, which was shown to be efficient in the treatment of MDR-TB (33, 34) and was recently recommended by WHO to be included in the treatment of MDR-TB, has a complex mode of action. In *M. smegmatis,* Yano et al. (19) showed that CFZ is a prodrug that is reduced by Ndh, and oxidation of reduced CFZ by oxygen generates reactive oxygen species. Since NdhA is not present in *M. smegmatis,* both enzymes, Ndh and NdhA, could be involved in the reduction of CFZ in *Mtb*. The MIC of CFZ was higher for Δ*ndh* but not for Δ*ndhA* compared with the WT *Mtb* strain, supporting the involvement of Ndh and not NdhA in the mechanism of action of CFZ.

This study underlines the critical role of the type I NADH dehydrogenase in *Mtb*. The loss of both *nuoAN* and *ndh* in *Mtb* resulted in the most pronounced phenotypes in terms of growth and virulence. Although this is not a true synthetic lethality, this work clearly demonstrates that both the type I and type II NADH dehydrogenases play overlapping roles in the homeostasis of NADH in the growth of *Mtb*. Further metabolic and biochemical studies will be required to elucidate the specificity of type I and type II NADH dehydrogenases' metabolic roles, although the growth and virulence attenuation of the Δ*ndh*Δ*nuoAN* mutant suggests that Nuo may be an Achilles heel in the in vivo metabolism of *Mtb*. The set of these mutants in both virulent and BSL2-safe *Mtb* strains should provide useful tools for screening of new compounds to disable the electron transport pathways of the tubercle bacilli.

Methods

Bacterial Strains. The *Mtb* strains, plasmids, and phages used in this study were obtained from laboratory stocks. mc^26230 (*Mtb* H37Rv ΔRD1Δ*panCD*) is an *Mtb* strain (35) reclassified as a biosafety level 2 strain by the Albert Einstein College of Medicine Institutional Biosafety Committee. The strains were grown at 37 °C in Middlebrook 7H9 (Difco), supplemented with 10% (vol/vol) OADC (oleic acid-albumin-dextrose-catalase; Difco), 0.2% (vol/vol) glycerol, 0.05% (vol/vol) tyloxapol. The solid media used were Middlebrook 7H10 (Difco), supplemented with 10% (vol/vol) OADC and 0.2% (vol/vol) glycerol. Plates were incubated at 37 °C for 4 to 8 wk. *D*-pantothenate (24 mg/L) was added to the liquid or solid media to grow mc^26230. The *ndh, ndhA,* and the full operon *nuoAN* were deleted from *Mtb* CDC1551 and mc^26230 using the specialized transduction system (14).

MICROBIOLOGY

Quantitative Real-Time PCR. *ndh, ndhA,* and *nuoH* relative expression was measured by quantitative real-time PCR (RT-qPCR). Triplicate cultures (10 mL) of *Mtb* CDC1551, CDC1551 Δ*ndh*, CDC1551 Δ*ndhA*, CDC1551 Δ*nuoAN*, CDC1551 Δ*ndh*Δ*nuoAN,* CDC1551 Δ*ndhA*Δ*nuoAN,* CDC1551 Δ*ndh* pMV361::*ndh*, and CDC1551 Δ*ndhA* pMV361::*ndhA* were grown to an $OD_{600\ nm} \approx 0.1$ at 37 °C and centrifuged, and the cell pellets were resuspended in 1 mL Qiagen RNA Protect reagent (Qiagen) for 24 h. RNA was isolated using Qiagen RNeasy kit, and RT-qPCR was performed using protocols previously described (36).

Measurement of NADH and NAD^+ Cellular Concentrations. Cultures (12 mL) were grown at 37 °C to log phase ($OD_{600\ nm} \approx 1.0$) in Middlebrook 7H9 medium (see above). NAD^+ and NADH were extracted as previously described (36), and their concentrations were obtained by measuring spectrophotometrically the rate of 3-[4,5-dimethylthiazol-2-yl]–2,5-diphenyltetrazolium bromide reduction by the yeast type II alcohol dehydrogenase in the presence of phenazine ethosulfate at 570 nm (37, 38).

Minimum Inhibitory Concentration Determination. The strains were grown to $OD_{600\ nm} \approx 0.8$–1 and diluted 1/1,000. Serial twofold dilutions of each drug tested were prepared in sterile 96-well plates for a final volume of 0.1 mL before the addition of the diluted bacterial cultures (0.1 mL). The plates were incubated at 37 °C for 7 d. $OD_{590\ nm}$ was read on a plate reader, and the MIC was determined as the lowest concentration of drug that prevented growth.

Murine Macrophage Infection. J774A.1 macrophage cells (ATCC) were subcultured according to the supplier's recommendations in Dulbecco's modified Eagle medium (DMEM; Invitrogen), supplemented with 10% FBS (Invitrogen). Macrophages (~100,000 cells per well) were seeded into 24-well tissue culture plates and cultured for 3 d. At the time of the infection, cell density was $\sim 3.6 \times 10^5$ cells per well. The *Mtb* strains were grown at 37 °C to $OD_{600\ nm} \approx 0.8$, washed twice in PBS, and sonicated twice for 10 s. The bacterial suspensions were diluted in DMEM, supplemented with 10% FBS, and used to infect the J774 cells for 4 h at 37 °C in 5% CO_2 at an approximate multiplicity of infection (MOI) of 1 to allow for bacterial uptake. Cell monolayers were washed twice with PBS and incubated in DMEM, supplemented with 10% FBS at 37 °C in 5% CO_2. At specific time points, media were removed, and the wells were washed once with PBS and then treated for 5 min with 0.05% aqueous SDS solution to lyse the macrophages. The lysates were serially diluted in PBS and plated for colony-forming unit (cfu) determination.

Mouse Challenge Experiments. The *Mtb* strains were grown to $OD_{600\ nm} \approx 0.8$, washed twice with PBS, sonicated (2×10 s), and diluted to the appropriate cell densities. C57BL/6 female mice (6–8 wk old) were obtained from the National Cancer Institute. For the i.v. infection, mice were infected with the *Mtb* strains ($\sim 1 \times 10^6$ cfu). Nine mice from each group were kept for the survival experiment. For the aerosol infection, mice were infected with a low dose (100–175 cfus per lung) of the *Mtb* strains used following a published protocol (39). For each experiment, at the indicated time point, mice were euthanized, and the spleens and right lungs were collected and homogenized in PBS containing 0.05% (vol/vol) tyloxapol. The organ lysates were plated on Middlebrook 7H10 plates to determine cfus per organ.

The animal protocol #20150215 "Evaluation of the safety and the efficacy of attenuated mycobacterial vaccine vectors" was approved by the Einstein Animal Institute, which is accredited by the "American Association for the Use of Laboratory Animals" [DHEW Publication No. (NIH) 78–23, Revised 1978] and accepts as mandatory the NIH "Principles for the Use of Animals."

More detailed methods are available in *Supporting Information*.

ACKNOWLEDGMENTS. We are grateful to Mei Chen and John Kim for technical assistance with the mice work. We thank Drs. Michael Berney and Gregory Cook for helpful discussions and critical reading of the manuscript.

1. Jnawali H, Ryoo S (2013) First- and second-line drugs and drug resistance. Available at https://www.intechopen.com/books/tuberculosis-current-issues-in-diagnosis-and-management/first-and-second-line-drugs-and-drug-resistance. Accessed January 20, 2018.
2. Pethe K, et al. (2013) Discovery of Q203, a potent clinical candidate for the treatment of tuberculosis. *Nat Med* 19:1157–1160.
3. Kalia NP, et al. (2017) Exploiting the synthetic lethality between terminal respiratory oxidases to kill *Mycobacterium tuberculosis* and clear host infection. *Proc Natl Acad Sci USA* 114:7426–7431.
4. Li K, et al. (2014) Multitarget drug discovery for tuberculosis and other infectious diseases. *J Med Chem* 57:3126–3139.
5. Cook GM, et al. (2017) Oxidative phosphorylation as a target space for tuberculosis: Success, caution, and future directions. *Microbiol Spectr* 5:TBTB2-0014-2016.
6. Sassetti CM, Boyd DH, Rubin EJ (2003) Genes required for mycobacterial growth defined by high density mutagenesis. *Mol Microbiol* 48:77–84.
7. Rao SP, Alonso S, Rand L, Dick T, Pethe K (2008) The protonmotive force is required for maintaining ATP homeostasis and viability of hypoxic, nonreplicating *Mycobacterium tuberculosis. Proc Natl Acad Sci USA* 105:11945–11950.
8. McAdam RA, et al. (2002) Characterization of a *Mycobacterium tuberculosis* H37Rv transposon library reveals insertions in 351 ORFs and mutants with altered virulence. *Microbiology* 148:2975–2986.
9. Miesel L, Weisbrod TR, Marcinkeviciene JA, Bittman R, Jacobs WR, Jr (1998) NADH dehydrogenase defects confer isoniazid resistance and conditional lethality in *Mycobacterium smegmatis. J Bacteriol* 180:2459–2467.
10. Vilchèze C, et al. (2005) Altered NADH/NAD+ ratio mediates coresistance to isoniazid and ethionamide in mycobacteria. *Antimicrob Agents Chemother* 49:708–720.
11. Griffin JE, et al. (2011) High-resolution phenotypic profiling defines genes essential for mycobacterial growth and cholesterol catabolism. *PLoS Pathog* 7:e1002251.
12. Awasthy D, Ambady A, Narayana A, Morayya S, Sharma U (2014) Roles of the two type II NADH dehydrogenases in the survival of *Mycobacterium tuberculosis* in vitro. *Gene* 550:110–116.
13. Bardarov S, et al. (2002) Specialized transduction: An efficient method for generating marked and unmarked targeted gene disruptions in *Mycobacterium tuberculosis, M. bovis* BCG and *M. smegmatis. Microbiology* 148:3007–3017.
14. Jain P, et al. (2014) Specialized transduction designed for precise high-throughput unmarked deletions in *Mycobacterium tuberculosis. MBio* 5:e01245-14.
15. Rolfe MD, et al. (2012) Lag phase is a distinct growth phase that prepares bacteria for exponential growth and involves transient metal accumulation. *J Bacteriol* 194:686–701.
16. Cuny C, Lesbats M, Dukan S (2007) Induction of a global stress response during the first step of *Escherichia coli* plate growth. *Appl Environ Microbiol* 73:885–889.
17. Vilchèze C, Hartman T, Weinrick B, Jacobs WR, Jr (2013) *Mycobacterium tuberculosis* is extraordinarily sensitive to killing by a vitamin C-induced Fenton reaction. *Nat Commun* 4:1881.
18. Yano T, Li LS, Weinstein E, Teh JS, Rubin H (2006) Steady-state kinetics and inhibitory action of antitubercular phenothiazines on *mycobacterium tuberculosis* type-II NADH-menaquinone oxidoreductase (NDH-2). *J Biol Chem* 281:11456–11463.
19. Yano T, et al. (2011) Reduction of clofazimine by mycobacterial type 2 NADH:quinone oxidoreductase: A pathway for the generation of bactericidal levels of reactive oxygen species. *J Biol Chem* 286:10276–10287.
20. Hards K, Cook GM (2018) Targeting bacterial energetics to produce new antimicrobials. *Drug Resist Updates* 36:1–12.
21. Velmurugan K, et al. (2007) *Mycobacterium tuberculosis nuoG* is a virulence gene that inhibits apoptosis of infected host cells. *PLoS Pathog* 3:e110.
22. Kaufmann SH, et al. (2014) The BCG replacement vaccine VPM1002: From drawing board to clinical trial. *Expert Rev Vaccines* 13:619–630.
23. Gengenbacher M, et al. (2016) Deletion of nuoG from the vaccine candidate Mycobacterium bovis BCG ΔureC:hly improves protection against tuberculosis. *MBio* 7:e00679-16.
24. Weinstein EA, et al. (2005) Inhibitors of type II NADH:menaquinone oxidoreductase represent a class of antitubercular drugs. *Proc Natl Acad Sci USA* 102:4548–4553.
25. Monod J (1949) The growth of bacterial cultures. *Annu Rev Microbiol* 3:371–394.
26. Hartman T, et al. (2014) Succinate dehydrogenase is the regulator of respiration in *Mycobacterium tuberculosis. PLoS Pathog* 10:e1004510.
27. Bald D, Villellas C, Lu P, Koul A (2017) Targeting energy metabolism in *Mycobacterium tuberculosis*, a new paradigm in antimycobacterial drug discovery. *MBio* 8:e00272-17.
28. Farhana A, et al. (2010) Reductive stress in microbes: Implications for understanding *Mycobacterium tuberculosis* disease and persistence. *Adv Microb Physiol* 57:43–117.
29. Hong WD, et al. (2017) Rational design, synthesis, and biological evaluation of heterocyclic quinolones targeting the respiratory chain of *Mycobacterium tuberculosis. J Med Chem* 60:3703–3726.
30. Rozwarski DA, Grant GA, Barton DH, Jacobs WR, Jr, Sacchettini JC (1998) Modification of the NADH of the isoniazid target (InhA) from *Mycobacterium tuberculosis*. *Science* 279:98–102.
31. Zhang Y, Heym B, Allen B, Young D, Cole S (1992) The catalase-peroxidase gene and isoniazid resistance of *Mycobacterium tuberculosis*. *Nature* 358:591–593.
32. Vilcheze C, Jacobs WR, Jr (2014) Resistance to isoniazid and ethionamide in Mycobacterium tuberculosis: Genes, mutations, and causalities. *Microbiol Spectr* 2:MGM2-0014-2013.
33. Tang S, et al. (2015) Clofazimine for the treatment of multidrug-resistant tuberculosis: Prospective, multicenter, randomized controlled study in China. *Clin Infect Dis* 60:1361–1367.
34. Van Deun A, et al. (2010) Short, highly effective, and inexpensive standardized treatment of multidrug-resistant tuberculosis. *Am J Respir Crit Care Med* 182:684–692.
35. Sambandamurthy VK, et al. (2006) *Mycobacterium tuberculosis* Delta*RD1* Delta*panCD*: A safe and limited replicating mutant strain that protects immunocompetent and immunocompromised mice against experimental tuberculosis. *Vaccine* 24:6309–6320.
36. Vilchèze C, Weinrick B, Wong KW, Chen B, Jacobs WR, Jr (2010) NAD^+ auxotrophy is bacteriocidal for the tubercle bacilli. *Mol Microbiol* 76:365–377.
37. Leonardo MR, Dailly Y, Clark DP (1996) Role of NAD in regulating the *adhE* gene of *Escherichia coli. J Bacteriol* 178:6013–6018.
38. San KY, et al. (2002) Metabolic engineering through cofactor manipulation and its effects on metabolic flux redistribution in *Escherichia coli. Metab Eng* 4:182–192.
39. Chen B, et al. (2011) Einstein contained aerosol pulmonizer (ECAP): Improved biosafety for multi-drug resistant (MDR) and extensively drug resistant (XDR) *Mycobacterium tuberculosis* aerosol infection studies. *Appl Biosaf* 16:134–138.